

Analysing NOx and soot formations of an annular chamber with various types of biofuels

Joanne Zi Fen Lim^a and Nurul Musfirah Mazlan*

School of Aerospace Engineering, Engineering Campus, Universiti Sains Malaysia,
14300 Nibong Tebal, Pulau Pinang, Malaysia

(Received August 28, 2022, Revised November 16, 2022, Accepted November 21, 2022)

Abstract. The rapid decrease of fossil fuel resources and increase of environmental pollution caused by aviation industries have become a severe issue which leads to an increase in the greenhouse effect. The use of biofuel becomes an option to alleviate issues related to unrennewable resources. This study presents a computational simulation of the biofuel combustion characteristics of various alternative fuels in an annular combustion chamber designed for training aircraft. The biofuels used in this study are Sorghum Oil Methyl Ester (SOME), Spirulina Platensis Algae (SPA) and Camelina Hydrotreated Esters and Fatty Acids (CHEFA). Meanwhile, Jet-A is used as a baseline fuel. The fuel properties and combustion characteristics are being investigated and analysed. The results are presented in terms of temperature and pressure profiles in addition to the formation of NOx and soot generated from the combustion chamber. Results obtained show that CHEFA fuel is the most recommended biofuel among all four tested fuels as it is being found that it burns with 37.6% lower temperature, 15.2% lower pressure, 89.5% lower NOx emission and 8.1% lower soot emission compared with the baseline fuel in same combustion chamber geometry with same initial parameters.

Keywords: annular chamber; biofuels; CFD simulation; emissions; NOx; soot

1. Introduction

Petroleum-based fuels are non-renewable resources which have been used in producing power for many applications. Unfortunately, high consumption of fuel in the transportation and power generation industries increases nitrogen oxides (NOx) and soot emissions, thus reducing the protective ozone layer in the stratosphere and provides a bad effect on human life. A significant amount of NOx gases are generated from the reaction of nitrogen and oxygen gaseous in the air during the combustion burning process, especially as the flame temperature reaches 2800°F (~1538°C) (Klapmeyer and Marr 2012, Zhang *et al.* 2012, Vennam *et al.* 2017). In aircraft, the high flame temperature occurs at high power settings such as during take-off which requires the aircraft to produce maximum power to encounter drag and provide enough lift to be in the air. In opposite, the formation of soot increases with the flame temperature. More soot is produced in the fuel-rich zone of the combustion chamber which is mainly close to the fuel spray region. Soot

*Corresponding author, Ph.D., E-mail: nmusfirah@usm.my

^aPh.D. Student

forms in this region will be passed to the end of the combustor and adversely affect the engine performance.

NOx is formed from three pathways: Thermal-NOx, Prompt-NOx and Fuel-NOx. The formation of NOx through the fuel-NOx pathway depends on the composition of a nitrogen molecule in the fuel. A small percentage of nitrogen in the fuel molecule does not contribute significantly to the NOx formation of the gas turbine. The formation of NOx is mainly dominated by prompt-NOx and thermal-NOx which the latest contributed mainly to the total formation of NOx. Rapid increases of thermal-NOx are related to increases in temperature and concentration of reactants as described by the chemical reactions known as Zeldovich mechanisms. Increment of prompt-NOx depends on the residence time where high temperature occurs and accumulates. NOx is generated from the reaction between the nitrogen gas and oxygen gas in the air during the burning process at high temperatures. NOx is normally formed when the flame temperature reaches 2800°F, which is about 1538°C (Sabnis and Aggarwal 2018). The prompt NOx formation occurred in rich flames which at the same time involved a series of complex reactions and intermediate species such as methylene (CH), dinitrogen (N₂) and hydrogen cyanide (HCN) (Watanabe *et al.* 2011). The prompt-NOx from the based flame is mostly formed by the CH reaction that controls the NOx formation rate as shown in equation 1 below (Fluent 2015).

$$\frac{d[NO]}{dt} = k_0[CH][N_2] \quad (1)$$

Where: k_0 = rate constant

Soot is an undesirable product from incomplete hydrocarbon (HC) combustion (Merker *et al.* 2005). Soot emitted into the atmosphere have caused health problems to human and the environment. The diameter of soot particles is less than 100 nm, which would easily travel deep into the lungs and into blood circulatory systems (Sabnis and Aggarwal 2018). The soot model can be performed by three different models, which are: the one-step soot model, the two-step soot model and the Moss-Brookes model. The one-step Khan and Greeves model is chosen in this study as it is valid for a wide range of hydrocarbon fuels, this model involved a single transport equation for soot mass fraction as shown in equation 2 below (Fluent 2015).

$$\frac{\partial}{\partial t}(\rho Y_{soot}) + \nabla \cdot (\rho \vec{v} Y_{soot}) = \nabla \cdot \left(\frac{\mu_t}{\sigma_{soot}} \nabla Y_{soot} \right) + R_{soot} \quad (2)$$

Where Y_{soot} indicates soot mass fraction, σ_{soot} indicates turbulent Prandtl number for soot transport and R_{soot} is net rate of soot generation (kg/m³-s).

An extensive study has been done on replacing geological processed fuel with renewable resources (Mark and Selwyn 2016, Ved and Padam 2013, Mostafa and El-Gendy 2017, Gawron and Białecky 2018). Biofuel is one of the common renewable resources that is capable to reduce the demand of fossil fuels and is more environmental friendly as it can alleviate greenhouse gases emission (Bhardwaj *et al.* 2015, Hari *et al.* 2015, Zhang and Chen 2015, Baharozu *et al.* 2017). The use of biofuels in aircraft reduces carbon particle emissions by 70% and decreases the formation of contrails, which are impacting the atmosphere adversely (Kumar 2017, Moore *et al.* 2017). The International Air Transport Association (IATA) has established the target of 10% use of biofuels which consistent with the goal of the industry's carbon footprint with a reduction of up to 80% in the years ahead (Moore *et al.* 2017). The use of biofuel has been implemented in the aerospace industry. For example, Airbus has become the first airplane manufacturer that provides the option of transporting their new jet by using blended sustainable jet fuel to its customers since

the first delivery in May 2016 (Sapp 2017).

The main concern of biofuel production from renewable resources is related to relatively low GHG's life cycle and sustainability at an economical price compared with other resources (Hari *et al.* 2015). Biofuel is compatible to provide both near-term and long-term solutions to the aviation industries with lower environmental impacts compared with fossil-based fuels (Wang *et al.* 2016). Biofuels are categorized into first (1G), second (2G), third (3G) and fourth (4G) generations. The 1G biofuels were initially produced from food crops such as corn, wheat, sugarcane and soybean (Mat Aron *et al.* 2020). However, the 1G biofuels are competing with food sources and consequently increase the food price and restrict their utilisation. The 2G biofuels are developed from wastes, residues and non-edible components. The lignocellulosic biomass has been used widely to develop 2G biofuels. The lignocellulosic biomass is inexpensive and found in abundance. However, the conversion process of the lignocellulosic biomass is harder than starch-based feedstock causing limitations to the use of 2G biofuels. The disadvantages of 1G and 2G biofuels leads to 3G biofuel production. The 3G biofuels are produced mainly from algae (Debnath *et al.* 2021) due to their various advantages such as rapid growth, requiring fewer nutrients to grow, and high-energy yield. Recently studies were conducted on 4G biofuel developed from microalgae (Debnath *et al.* 2021) and genetically modified microalgae (Mat Aron *et al.* 2020, Godbole *et al.* 2021, Shokravi *et al.* 2021). The modification to the microalgae genetics has increased lipid and carbohydrate content in microalgae thus improving biofuel yield (Shokravi *et al.* 2021).

As far as biofuels are concerned, many studies have been performed to predict the characteristics of biofuel combustion as summarized in Table 1. Most of the studies on biofuel combustion were performed experimentally. Meanwhile, the capability and reliability of computational fluid dynamics (CFD) in measuring combustion performance is well-known. Based on Table 1, it is observed that most of the CFD simulation was performed mainly for Jet-A fuel. Additionally, most of the experimental works related to biofuels were only focusing on temperature, pressure, velocity and NO_x formation. The formation of soot from biofuel combustion was lacking in the literature. Therefore, this study aims to measure the formation of NO_x and soot as well as other combustion characteristics such as pressure and temperature profiles through the incorporation of various types of biofuels from a different generation in the similar combustor geometry designed in Mark and Selwyn (2016). The combustion parameters measured in this present study were also expanded by exploring the impact of these varieties of biofuel generation on NO_x and soot formation.

2. Materials and methods

2.1 Fuel types

Three types of biofuels were evaluated in this present study which is Sorghum Oil Methyl Ester (SOME), Spirulina Platensis Algae (SPA) and Camelina Hydrotreated Esters and Fatty Acids (CHEFA). The SOME has a higher viscosity, specific gravity, flash point, pour point, cloud point, lesser density and acid value when compared to conventional diesel fuel (Ved and Padam 2013). The SPA is an algae type of fuel investigated in Mostafa *et al.* (Mostafa and El-Gendy 2017). When the algae blend with diesel fuel, the viscosity, density, total acid number, initial boiling point, calorific value, flash point, cetane number and diesel index increase, while the pour point,

Table 1 Summary of biofuels studies from several researchers

No	Researchers	Methods of study	Feedstock	Parameters measured of the combustion product
1	Mark and Selwyn (2016)	CFD Simulation	Jet-A	Temperature Pressure Velocity
2	Rodrigo <i>et al.</i> (2017)	CFD Simulation	Biomass	Temperature Pressure Velocity NOx
3	Singh <i>et al.</i> (2017)	CFD Simulation and Experiment	Biodiesel (Vegetable Seed Oil)	Temperature Pressure Velocity NOx
4	Čerňan <i>et al.</i> (2017)	Experiment	FAME blended with Jet A-1 Fuel (0% to 100%)	NOx Soot
5	Cîrciu <i>et al.</i> (2015)	CFD Simulation	Jet-A fuel	Temperature Pressure Velocity
6	Zhang <i>et al.</i> (2012)	CFD Simulation	Jet-A fuel	Temperature Velocity NOx Soot
7	Zuber <i>et al.</i> (2017)	CFD Simulation	Jet-A fuel	Temperature Velocity NOx Soot
8	Ved and Padam (2013)	Experiment	Biodiesel (Sorghum oil)	Temperature
9	Mostafa and El-Gendy (2017)	Experiment	Algae Fuel (Spirulina Platensis) and Diesel (B2, B5, B10, and B20)	NOx Soot
10	Gawron and Bialecki (2018)	Experiment	CHEFA (Camelina Vegetable Oil) and Jet A-1 Fuel	Temperature Pressure Velocity NOx
11	Hui <i>et al.</i> (2012)	Experiment	Jet-A fuel, SPK fuels and HRJ fuels	Pressure Velocity
12	Gawron <i>et al.</i> (2020)	Experiment	Jet A-1 and CHEFA (Camelina oil plant blend and UCO blend)	Temperature Pressure NOx Soot

Table 2 Fuel properties of tested fuels

Fuel properties	Jet-A	SOME (Ved and Padam 2013)	SPA (Mostafa and El-Gendy 2017)	CHEFA (Gawron and Bialecki 2018)
Density (g/cm ³)	0.8	0.91	0.86	0.78
Viscosity (mm ² /s)	4.77	3.24	12.4	5.00
Specific Heat Capacity (kJ/g.°C)	42.80	43.00	31.50	43.70
Flash Point (°C)	38	225.00	189	66
Total Acid Number (mg)	0.01	0.43	0.75	0.35
No. of carbon atom	11-13	8 - 10	18	35
H/C ratio	5.56	4.00	4.76	3.03

cloud point, carbon residue and sulphur, ash and water contents decreased. The CHEFA was obtained from Gawron and Bialecki (2018). CHEFA has a higher viscosity, lower density, aromatics and heat of combustion when compared with the chosen conventional Jet A-1 fuel. CHEFA has been used as a “drop-in” with Jet-A. However, for evaluation purposes in this present study, only the properties of the fuel were taken from the literature. The properties of each fuel were shown in Table 2.

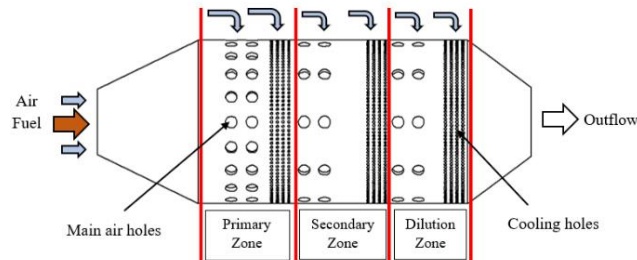


Fig. 1 The combustion schematic diagram according to Mark and Selwyn (2016)

Table 3 Dimensions of combustion chamber

Parameter	Value
Total length (m)	0.15719
Length of PZ (m)	0.03020
Length of SZ (m)	0.02013
Length of DZ (m)	0.06933
Body Diameter (m)	0.05649
Inlet Diameter (m)	0.02269
Outlet Diameter (m)	0.02374
Fuel Inlet Diameter (m)	0.00259
Wall Thickness (m)	0.00100
PZ Main Air Holes (No. of holes=40)	$1.257e^{-5} \text{ m}^2/\text{hole}$
SZ Main Air Holes (No. of holes=20)	$1.257e^{-5} \text{ m}^2/\text{hole}$
DZ Main Air Holes (No. of holes=20)	$1.256e^{-5} \text{ m}^2/\text{hole}$
PZ Cooling Holes (No. of holes=480)	
SZ Cooling Holes (No. of holes=600)	$3.181e^{-7} \text{ m}^2/\text{hole}$
DZ Cooling Holes (No. of holes=600)	

2.2 Combustion chamber modelling

The combustion chamber considered in this study was modelled based on an annular chamber designed for a low bypass turbofan engine in jet trainer aircraft as shown in Fig. 1. The annular chamber was chosen due to its advantages compared to the turbo-annular chamber as described in Yi *et al.* (2009). The chamber is divided into three zones known as the primary zone (PZ), secondary zone (SZ) and dilution zone (DZ). Each zone is provided with main and cooling holes. The PZ is a region of lower velocity recirculation and provides stable combustion (Filla 2012). The fuel was ignited when the temperature reaches a flash point and combusted in PZ. In the SZ, the fuel will react with primary air to form a toroidal vortex that stabilizes and anchor the flame. The additional amount of air in the SZ is the main cause of the formation of pollutants. Therefore, the temperature needs to be decreased steadily in this zone. DZ is a zone in which a large amount of cooling air enters the combustion to reduce the temperature before entering the turbine sections (Dhamale *et al.* 2011). This is to ensure the temperature of the combustion gases does not cause damage to the turbine blade. The combustion chamber modelled in Mark and Selwyn (2016) was simplified by assuming no casing covers the chamber. The design parameter and the important

equations of the annular combustion chamber model design are shown in Table 3.

2.3 Mesh independence analysis

Mesh independence analysis was performed to obtain reliable results. The chamber was meshed using unstructured tetrahedron mesh due to its flexibility to mesh complex geometry (Niesłony *et al.* 2015). The mesh was performed with linear element order. The minimum size of mesh was set as $8.43e^{-5}$ m, maximum face size of $8.43e^{-3}$ m, maximum element size of $1.69e^{-2}$ m, and the defeature size of $4.22e^{-5}$ m. The transition ratio of the meshing is 0.272, with maximum layer inflation of 5, a growth rate of 1.2, and a wall Y+ value of 100. Table 4 shows the mesh independence analysis performed for three types of mesh, course mesh (relevance centre: -100), medium mesh (relevance centre: 0) and fine mesh (relevance centre: +100).

2.4 Boundary conditions

The combustion chamber has air inlets, a fuel inlet, PZ main holes inlet (Main1), SZ main holes inlet (Main2), DZ main holes inlet (Main3), PZ cooling holes inlet (Cooling1), SZ cooling holes inlet (Cooling2) and DZ cooling holes inlet (Cooling3). The amount of air entering the chamber is depicted in Table 5 as suggested by (Mark and Selwyn 2016).

Based on the observation, the course mesh (2,300,563 mesh grid) as shown in Fig. 2 is chosen to be used in all simulations because of the small percentage difference between all types of mesh and the lowest execution time, which is about 8 hours for 100 iterations. The simulation running is done by the laptop with Intel(R) Core (TM) i7-8750H CPU @ 2.20GHz processor, 8GB installed RAM and 64-bit operating system.

To study the impact of fuel properties on combustion characteristics, the initial parameter and the selection of the turbulence model in FLUENT are set to be constant for each fuel. The initial parameters of air mass flow, fuel flow and operating condition were obtained from Mark and Selwyn (2016) and kept constant for each fuel. The air temperature and air pressure were set as

Table 4 Mesh independence analysis of the combustion chamber

Mesh	No. of elements	Reference temperature (K)	Duration to complete simulation (hrs)	Percentage different with Literature (%)
Density (g/cm^3)	2,300,563		8	2.09
Viscosity (mm^2/s)	7,971,272	743	12	17.4
Specific Heat Capacity ($\text{kJ}/\text{g}\cdot^\circ\text{C}$)	31,001,964		20	96.7

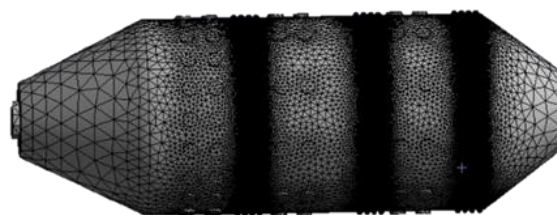
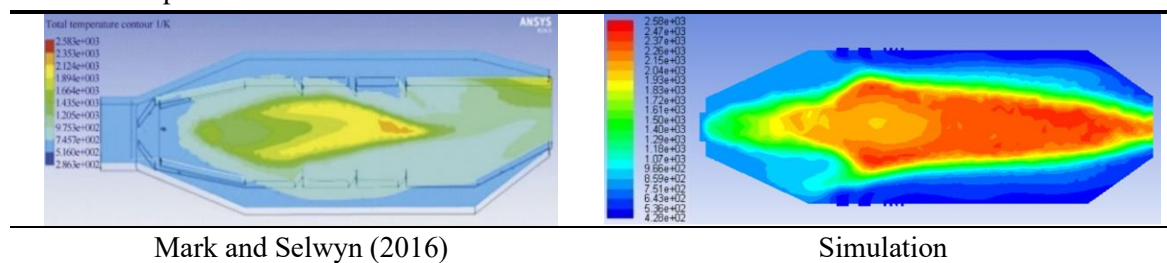


Fig. 2 The combustion schematic diagram according to Mark and Selwyn (2016)

Table 5 Distribution of the airflow and fuel flow in the combustion chamber

Parameter	Airflow distribution (%)	Air mass flow rate (kg)
Air inlet	20	5.74
PZ main holes	20	5.74
SZ main holes	10	2.87
DZ main holes	10	2.87
PZ cooling holes	11.4	3.27
SZ cooling holes	14.3	4.11
DZ cooling holes	14.3	4.11
Fuel	-	0.92

Table 6 Comparison between combustion chamber model with literature



743.352 K and 2 atm respectively. The fuel was not pre-heated and set to 287 K. The energy equation and species transport were considered. The simulation was performed in a steady state. The combustion model was non-premixed as the fuel and air entered the chamber from a separate pathway. The eddy-dissipation method was chosen for the turbulence-chemistry interaction. The eddy-dissipation method allowed the fuel and oxidizer to mix homogeneously in the reaction zone (Magnussen 2005, Fluent 2015) The k-epsilon viscous model was chosen as its mechanism can be applied to a large number of turbulent applications including combustion process (Mohammadi and Pironneau 1993, Fluent 2015).

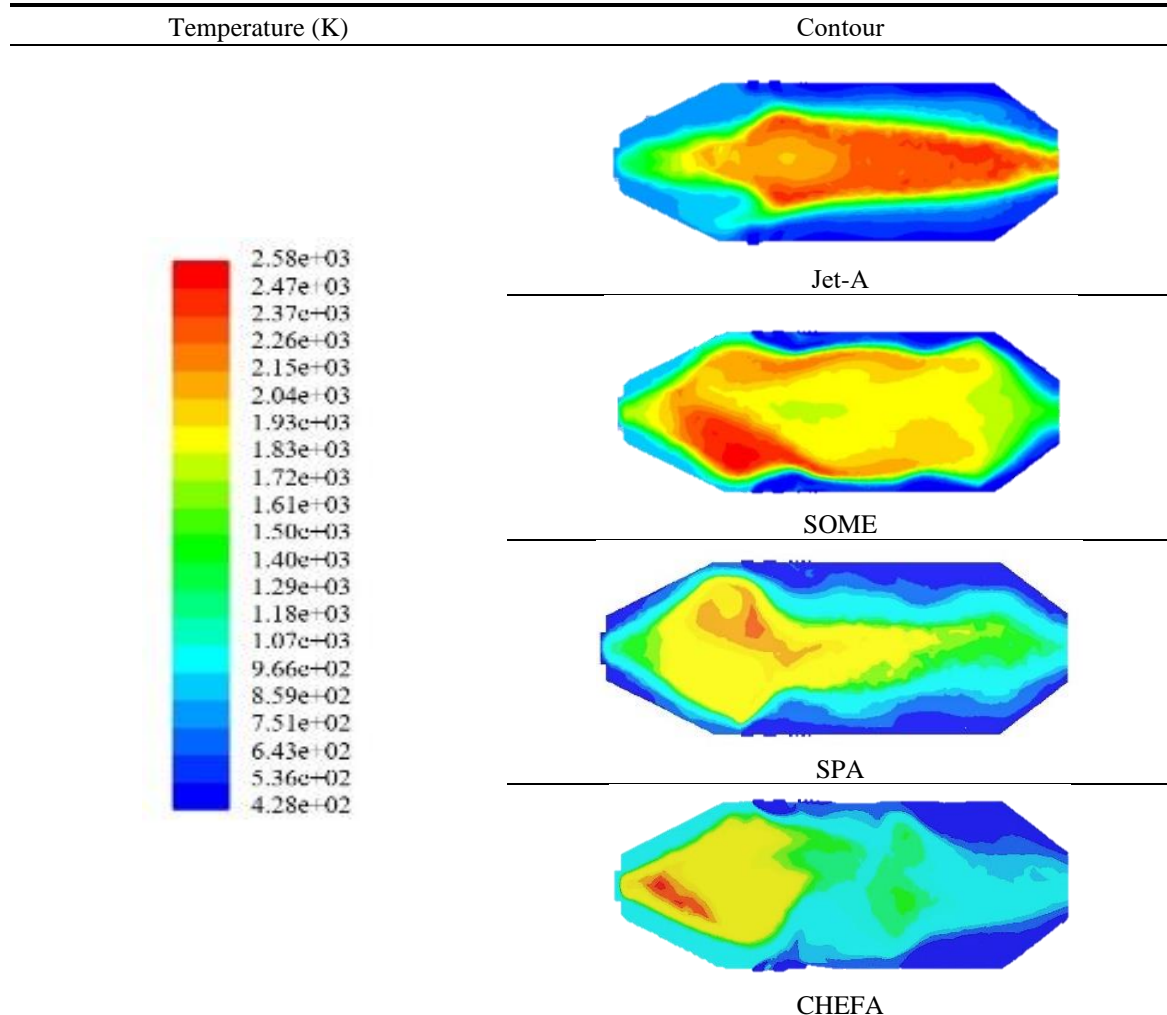
Thermal-NO_x and prompt-NO_x were selected to evaluate NO_x emission. The temperature variance was set as the transported temperature to obtain the result of pollutant NO_x with temperature variance. A one-step soot model in the boundary condition was selected to evaluate soot formation as suggested in Cheng *et al.* (2008). The one-step soot model is already sufficient for a wide range of hydrocarbon fuels. In the soot formation setting, the fuel species such as density and viscosity according to Table 2 were used and the O₂ was set for the oxidant. The convergence criteria of 10⁻⁶ were set for the simulation.

3. Results and discussion

3.1 Model validation

The model was first validated by comparing the present simulation with Mark and Selwyn (2016) who evaluated Jet-A in their work. K-epsilon viscous model is used for the evaluation. Table 6 shows the comparison of total temperature between the literature and the simulation.

Table 7 Comparison of temperature contour



The maximum flame temperature of the present simulation is 11.86% higher than the maximum flame temperature obtained in the literature. The difference is expected due to the inconsideration of cold air trapped inside the chamber casing as considered in Mark and Selwyn (2016).

3.2 Comparison of temperature contour

Table 7 shows the temperature contours of Jet-A, SOME, SPA and CHEFA combustion. The temperature increases from the combustor inlet and decreases at the exit. It is observed that the location of the maximum flame temperature of the fuels is varied depending on the fuel type. The maximum temperature of Jet-A reaches a maximum flame temperature at the secondary zone, while the biofuels achieve maximum combustion temperature at the primary zone.

At the same inlet conditions, all biofuels produce lower flame temperatures compared to baseline fuel. The combustion temperature of SOME, SPA and CHEFA are 8%, 19.0% and 28.8%

lower than Jet-A respectively. The H/C ratio is found to influence the flame temperature. It is observed that fuel with a higher H/C ratio produces higher flame temperature. Jet-A with the highest H/C ratio, which is 5.56 is found to reach the highest flame temperature during combustion. The chemical energy produced from the combustion process is converted into output power of the combustion chamber, therefore, fuels with high carbon content will be producing high output power (Bartoňová 2015). Besides the H/C ratio, the viscosity of fuels leads to the amount of fuel injected into the chamber and spray patternation. Fuel with lower viscosity contributed to the short ignition delay and early injection timing then finally cause to higher combustion temperature (Won *et al.* 2019). Jet-A has a lower viscosity than biofuels resulting in a higher speed of fuel injection compared to biofuels which have high viscosity that will affect the injected fuel quantity and injection timing (Rodrigues *et al.* 2007, Won *et al.* 2019).

In addition to lower flame temperature, at the same amount of cooling air supplied to the chamber, combusting biofuels resulted to lower combustor outlet temperature compared to Jet-A. The SOME, SPA and CHEFA recorded 26.9%, 45.0% and 57.7% lower combustion outlet temperature compared to Jet-A. The lower temperature at the combustor outlet will prolong the turbine blade lifetime and lengthen the engine life.

3.3 Comparison of pressure contour

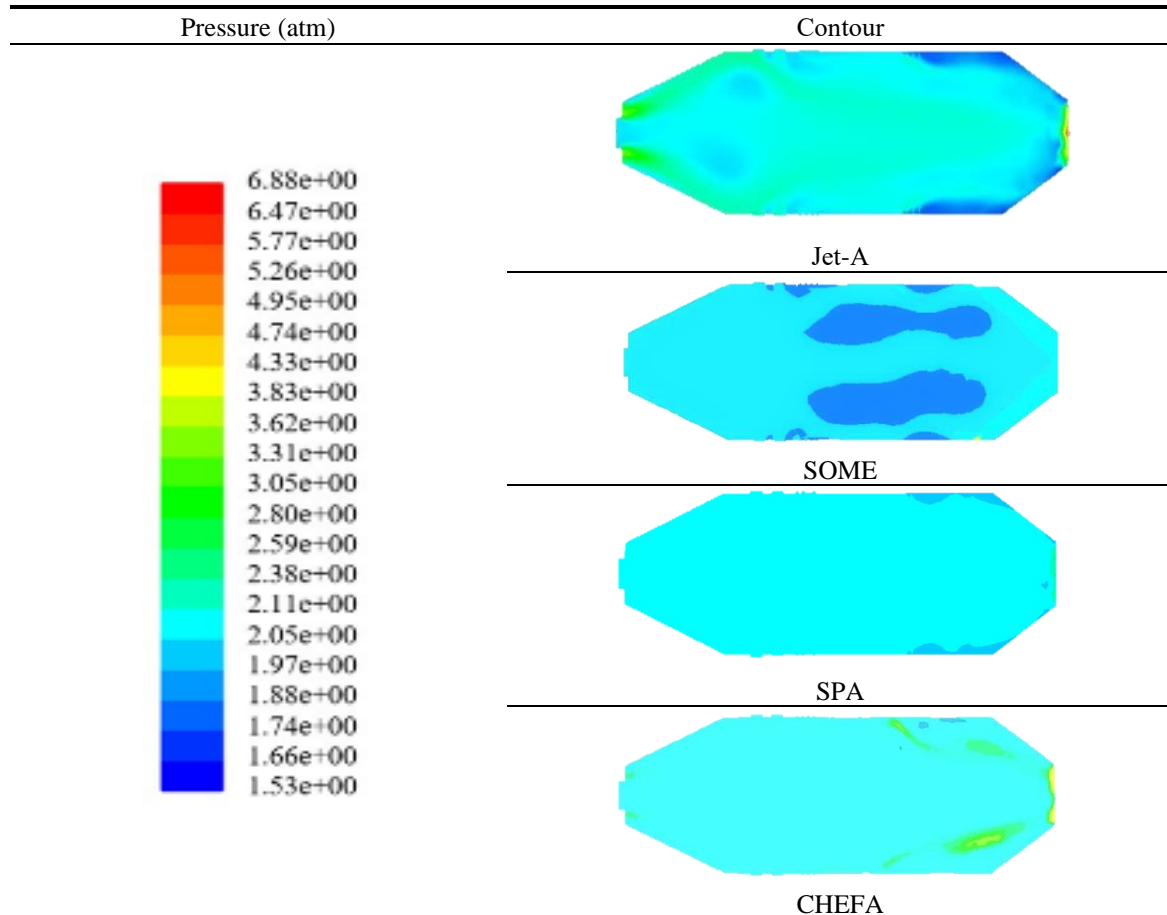
The comparison of pressure between Jet-A and biofuels is shown in Table 8. The initial inlet pressure for all fuels was set as 2 atm. Once the combustion occurred, an increment in total pressure was observed. The total pressure of Jet-A fuel is higher than biofuels. The average total pressure of the Jet-A fuel is 26.4% higher when compared to SOME, 18.2% higher when compared to SPA fuel, and 15.2% higher when compared to CHEFA. At the same time, the outlet pressure of the Jet-A fuel is 49.4% higher when compared to SOME, 31.5% higher when compared to SPA fuel, and 20.3% higher when compared to CHEFA. As a result of the highest average pressure and outlet pressure of the combustion chamber, a high regression rate and high combustion efficiency can be obtained (Kumar and Ramakrishna 2014). Meanwhile, the lower pressure obtained from biofuel combustion would lead to lower output energy produced (Meloni 2013, Funke *et al.* 2014).

As the fuel enters the combustion chamber and is heated, the temperature of the combustion gases increases hence increasing the volume of the air inside the chamber. The high temperature causes the expansion of the gaseous inside the combustion chamber. Due to the enclosed region of the combustion chamber, the available volume inside the chamber is fixed. As a result, the gaseous atoms are bouncing off with more energy and vigorous. Thus, the high speed of gas atoms causes an increase in pressure. The increase of total pressure in the combustion chamber increases the cracking reactions of high molecular weight fraction persisting in the liquid state and causing the increment of the speed of gaseous atoms (Cataluna and Da Silva 2012). This is the reason, the annular combustion chamber works with higher pressure and temperature to produce higher output energy (Merker *et al.* 2005, Rodrigues *et al.* 2007, Coogan *et al.* 2014).

3.4 Comparison of NO_x formation

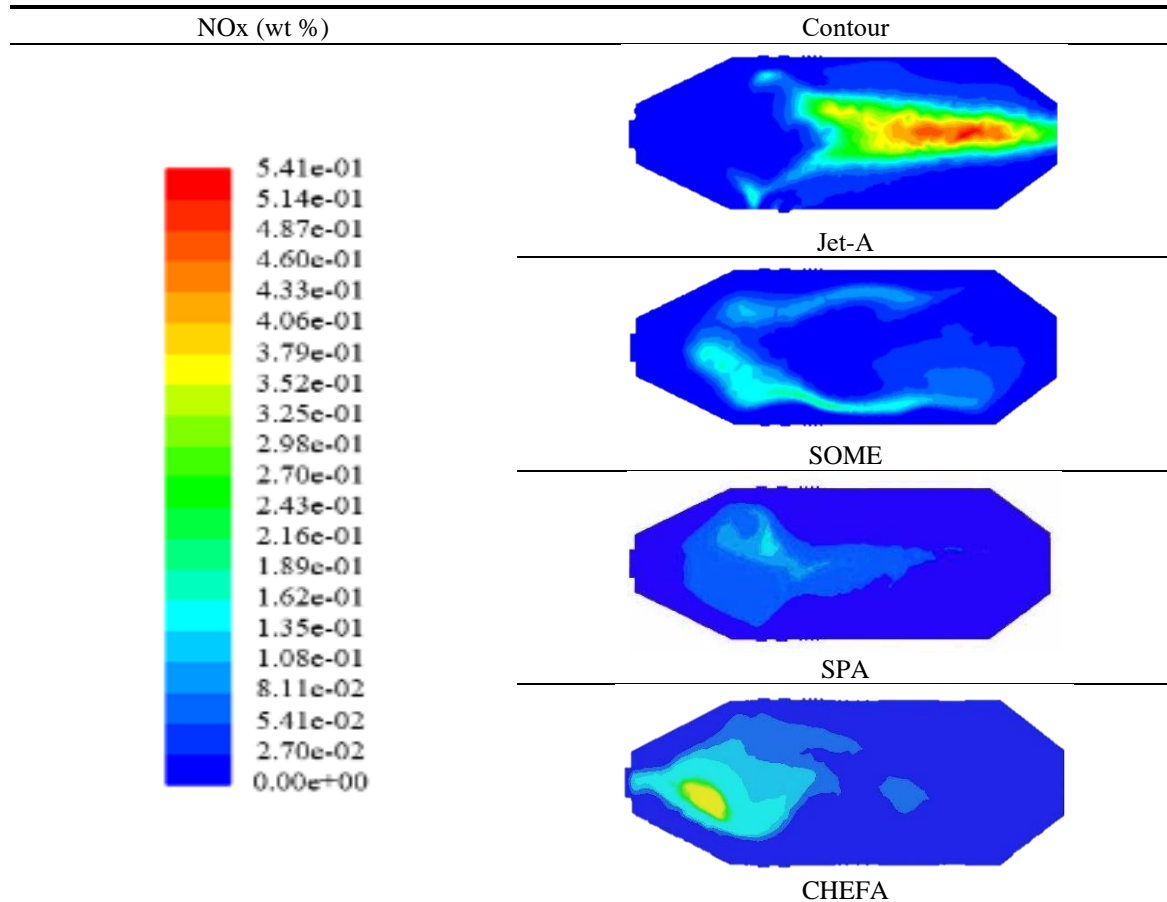
Table 9 shows the comparison of NO_x formation between Jet-A and biofuels. As far as the thermal-NO_x is concerned, the NO_x contours for all tested fuels have the same trend as the temperature contours. The formation of NO_x is high in the high-temperature region. SPA produces

Table 8 Comparison of pressure contour



the lowest NO_x emission compared to SOME and CHEFA, due to its low carbon content and high viscosity of the fuel. The carbon content of the fuel is about 18 carbon chains and the viscosity of the fuel is 12.4 mm²/s. The observation is consistent with results in Slade and Bauen (2013). The SOME, SPA and CHEFA produce 48.3%, 84.5% and 75.9% lower NO_x formation than the Jet-A fuel, respectively. The concentration of NO_x produced from the Jet-A has located downstream of the chamber while the NO_x is formed in the upstream region for biofuels. Although Jet-A has the best performance amongst the fuel due to the highest temperature and pressure, the NO_x emission of Jet-A fuel is the highest which is consequently harmful to the environment and humans. The formation of NO_x contributed by Jet-A is high in the secondary zone which corresponds to the high flame temperature region observed in Table 9. Meanwhile, burning SOME produces the lowest pressure due to its highest density and lowest viscosity compared to other fuels. As a result, SOME produces higher NO_x at the primary zone and drops instantaneously in the secondary zone and dilution zone. SPA provides the lowest NO_x as a result of the lowest pressure and temperature. However, the formation of NO_x at the secondary zone due to the highest viscosity of the fuel delays the combustion process as a result of larger droplets injected into the chamber (Singh and Gu 2010, Da Silva *et al.* 2011). Although CHEFA has the lowest density, the fuel has a

Table 9 Comparison of NOx contour

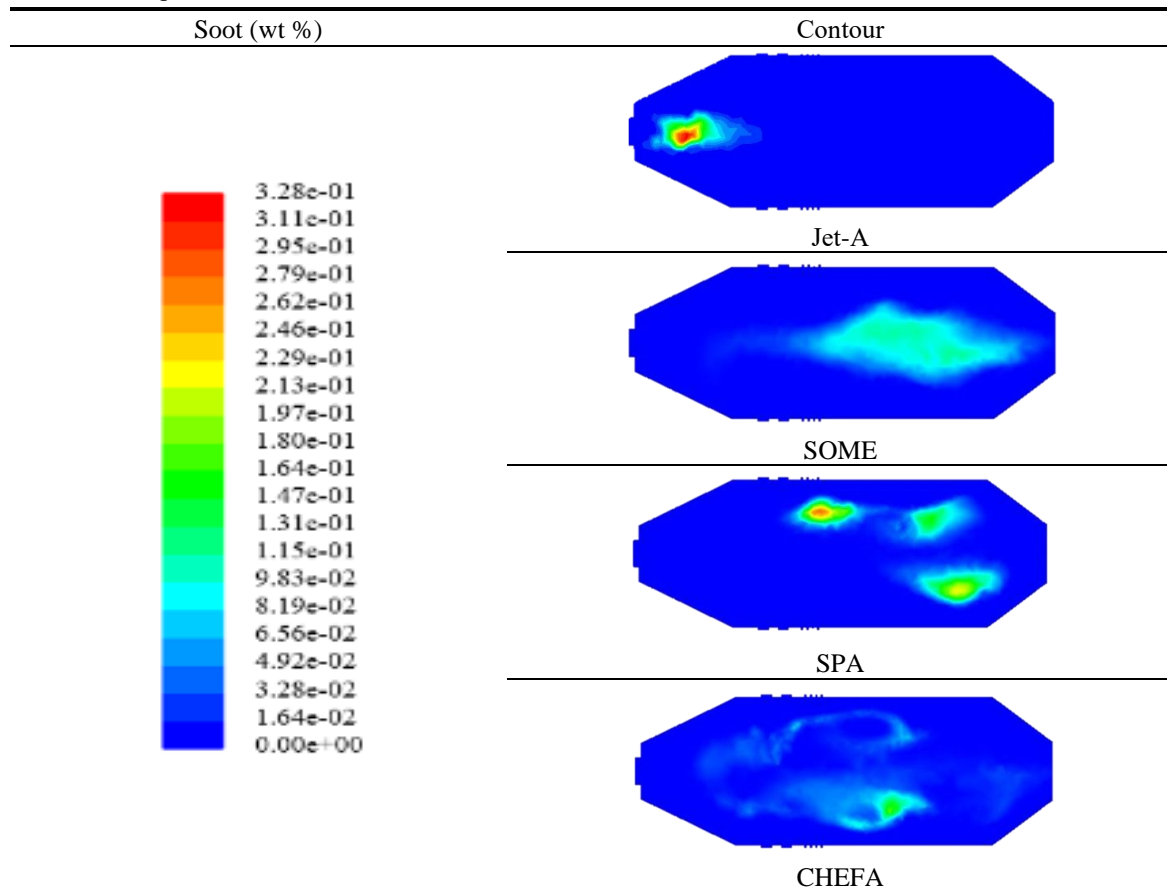


high viscosity which produces the lowest temperature but high pressure, and the NOx emission from CHEFA is relatively low compared to other fuels. The NOx emission of CHEFA fuel concentrates at the primary zone as the fuel burnt mostly in the primary zone. Fuel runs with high pressure and low temperature causes high output energy and low NOx emission (Hileman *et al.* 2008).

3.5 Comparison of soot formation

Soot is formed from the incomplete combustion of hydrocarbon fuel (Merker *et al.* 2005, Wang and Chung 2019). The lower combustion temperature is found to influence the soot formation where incomplete combustion occurs. The soot causes greenhouse gas effects and severe health problems, especially when related to the respiratory system (Bockhorn 2013). Hence, fuels burnt with low soot emissions are essential when considering an environmentally friendly fuel for the aviation industry. Table 10 shows the soot formation of Jet-A and biofuels. It is noticed that the soot emission for all tested fuels in the annular combustion chamber formed at the lower temperature region where the mass fraction of the oxygen is lacking to oxidize the soot. The soot

Table 10 Comparison of soot contour



formation of the Jet-A is accumulated at the primary zone, while the soot is formed at secondary and dilution zones for biofuels consistent with the low-temperature region observed in Table 10. The highest soot emission of SOME is 93.4% lower than the Jet-A fuel, soot emission of SPA fuel is 22.3% lower than the Jet-A fuel, and soot emission of CHEFA is 50.3% lower than the Jet-A fuel. As soot is the residual degraded carbon particles obtaining from incomplete burning of hydrocarbons, this simulation proves that the SOME contains the least H/C compounds among all tested fuels that run in this combustion chamber.

4. Conclusions

In conclusion, the tested fuels are comparing in the same combustion chamber geometry and similar initial parameters to determine the best alternative for the current Jet-A fuel as an alternative aviation fuel. According to the four perspectives of comparison, CHEFA has excellent performance compared to other fuels as it produces a relatively higher amount of output power and at the same time can lessen greenhouse gas emissions. The combustion of CHEFA produces the total pressure of 15.2% lower than the Jet-A fuel, which indicates a higher output power compared

to SOME and SPA fuels. Although the Jet-A is capable to combust with the highest temperature and pressure, the highest NO_x and soot produced are intolerable. The production of higher NO_x correlates with higher temperature produces from the combustion process. In addition, the highest combustion temperature of Jet-A is located at the dilution zone compared to CHEFA which has highest combustion temperature at the primary zone. The difference in the fuel properties has affected the fluid flow in the chamber. As far as the formation of NO_x is concerned, CHEFA produces 75.9% lower NO_x and 50.3% lower soot emissions compared to Jet-A, which is proven more environmentally friendly than the baseline fuel. On the other hand, burning SOME produces the least combustion efficiency whilst combusting SPA results in low energy produced. Therefore, CHEFA is the best alternative among the tested fuels in this study.

Acknowledgments

The authors would like to acknowledge Ministry of Higher Education Malaysia, grant number FRGS/1/2019/TK07/USM/03/5 and Graduate Fellowship USM (GFUSM) for the financial support.

References

- Baharozu, E., Soykan, G. and Ozerdem, M.B. (2017), "Future aircraft concept in terms of energy efficiency and environmental factors", *Energy*, **140**, 1368-1377. <https://doi.org/10.1016/j.energy.2017.09.007>.
- Bartoňová, L. (2015), "Unburned carbon from coal combustion ash: An overview", *Fuel Pr. Technol.*, **134**, 136-158. <https://doi.org/10.1016/j.fuproc.2015.01.028>.
- Bhardwaj, A.K., Zenone, T. and Chen, J. (2017), *Sustainable Biofuels*, De Gruyter, Berlin, Boston.
- Bockhorn, H. (2013), *Soot Formation in Combustion: Mechanisms and Models*, Springer Science & Business Media.
- Cataluna, R. and Da Silva, R. (2012), "Effect of cetane number on specific fuel consumption and particulate matter and unburned hydrocarbon emissions from diesel engines", *J. Combust.*, **2012**, Article ID 738940. <https://doi.org/10.1155/2012/738940>.
- Čerňan, J., Hocko, M. and Čúttová, M. (2017), "Safety risks of biofuel utilization in aircraft operations", *Transp. Res. Procedia*, **28**, 141-148. <https://doi.org/10.1016/j.trpro.2017.12.179>.
- Cheng, X., Jv, H. and Wu, Y. (2008), "Application of a phenomenological soot model for diesel engine combustion", *Internal Combustion Engine Division Spring Technical Conference*, **48132**, 205-214.
- Cîrciu, I., Rotaru, C., Luculescu, D. and Constantinescu, C. (2015), "Aircraft engine combustion chamber performances-numerical evaluation", *Appl. Mech. Mater.*, **811**, 167-171.
- Coogan, S., Brun, K. and Teraji, D. (2014), "Micromix combustor for high temperature hybrid gas turbine concentrated solar power systems", *Energy Procedia*, **49**, 1298-1307. <https://doi.org/10.1016/j.egypro.2014.03.139>.
- Da Silva, N.D.L., Batistella, C.B., Maciel Filho, R. and Maciel, M.R.W. (2011), "Investigation of biofuels properties", *Chem. Eng.*, **25**, 85.
- Debnath, C., Bandyopadhyay, T.K., Bhunia, B., Mishra, U., Narayanasamy, S. and Muthuraj, M. (2021), "Microalgae: Sustainable resource of carbohydrates in third-generation biofuel production", *Renew. Sustain. Energy Rev.*, **150**, 111464. <https://doi.org/10.1016/j.rser.2021.111464>.
- Dhamale, N., Parthasarathy, R.N. and Gollahalli, S.R. (2011), "Effects of turbulence on the combustion properties of partially premixed flames of canola methyl ester and diesel blends", *J. Combust.*, **2011**, Article ID 697805. <https://doi.org/10.1155/2011/697805>.

- Filla, R. (2012), "Representative testing of emissions and fuel consumption of working machines in reality and simulation", *Proceedings of the SAE 2012 Commercial Vehicle Engineering Congress*, Rosemont, IL, USA.
- Fluent, A. (2015), "Ansys fluent", Academic Research, Release, 14,
- Funke, H.W., Dickhoff, J., Keinz, J., Ayed, A.H., Parente, A. and Hendrick, P. (2014), "Experimental and numerical study of the micro mix combustion principle applied for hydrogen and hydrogen-rich syngas as fuel with increased energy density for industrial gas turbine", *Appl. Energy Procedia*, **61**, 1736-1739. <https://doi.org/10.1016/j.egypro.2014.12.201>.
- Gawron, B. and Bialecki, T. (2018), "Impact of a Jet A-1/HEFA blend on the performance and emission characteristics of a miniature turbojet engine", *Int. J. Environ. Sci. Technol.*, **15**(7), 1501-1508. <https://doi.org/10.1007/s13762-017-1528-3>.
- Gawron, B., Bialecki, T., Janicka, A. and Suchocki, T. (2020), "Combustion and emissions characteristics of the turbine engine fueled with HEFA blends from different feedstocks", *Energi.*, **13**(5), 1277. <https://doi.org/10.1007/s13762-017-1528-3>.
- Godbole, V., Pal, M.K. and Gautam, P. (2021), "A critical perspective on the scope of interdisciplinary approaches used in fourth-generation biofuel production", *Algal Res.*, **58**, 102436. <https://doi.org/10.1016/j.algal.2021.102436>.
- Hari, T.K., Yaakob, Z. and Binitha, N.N. (2015), "Aviation biofuel from renewable resources: routes, opportunities and challenges", *Renew. Sustain. Energy Rev.*, **42**, 1234-1244. <https://doi.org/10.1016/j.rser.2014.10.095>.
- Hileman, J., Katz, J.B., Mantilla, J.G. and Fleming, G. (2008), "Payload fuel energy efficiency as a metric for aviation environmental performance", *International Congress of Aeronautical Sciences*, September.
- Hui, X., Kumar, K., Sung, C.J., Edwards, T. and Gardner, D. (2012), "Experimental studies on the combustion characteristics of alternative jet fuels", *Fuel*, **98**, 176-182. <https://doi.org/10.1016/j.fuel.2012.03.040>.
- Klapmeyer, M.E. and Marr, L.C. (2012), "CO₂, NO_x, and particle emissions from aircraft and support activities at a regional airport", *Environ. Sci. Technol.*, **46**(20), 10974-10981. <https://doi.org/10.1021/es302346x>.
- Kumar, K. (2017), *Biofuels Can Reduce Aircraft Particle Emissions And Contrails: NASA Study*, Tech Times.
- Kumar, R. and Ramakrishna, P.A. (2014), "Measurement of regression rate in hybrid rocket using combustion chamber pressure", *Acta Astronautica*, **103**, 226-234. <https://doi.org/10.1016/j.actaastro.2014.06.044>.
- Magnussen, B.F. (2005), "The eddy dissipation concept: A bridge between science and technology", *ECCOMAS Thematic Conference on Computational Combustion*, Lisbon, Portugal.
- Mark, C. P. and A. Selwyn (2016), "Design and analysis of annular combustion chamber of a low bypass turbofan engine in a jet trainer aircraft", *Propuls. Power Res.*, **5**(2), 97-107. <https://doi.org/10.1016/j.jprr.2016.04.001>.
- Mat Aron, N.S., Khoo, K.S., Chew, K.W., Show, P.L., Chen, W.H. and Nguyen, T.H.P. (2020), "Sustainability of the four generations of biofuels-A review", *Int. J. Energy Res.*, **44**(12), 9266-9282. <https://doi.org/10.1002/er.5557>.
- Meloni, R. (2013), "pollutant emission validation of a heavy-duty gas turbine burner by CFD modeling", *Mach.*, **1**(3), 81-97. <https://doi.org/10.3390/machines1030081>.
- Merker, G.P., Schwarz, C., Stiesch, G. and Otto, F. (2005), *Simulating Combustion: Simulation of Combustion and Pollutant Formation for Engine-Development*, Springer Science & Business Media.
- Mohammadi, B. and Pironneau, O. (1993), *Analysis of the k-Epsilon Turbulence Model*, Paris.
- Moore, R.H., Thornhill, K.L., Weinzierl, B., Sauer, D., D'Ascoli, E., Kim, J., ... & Anderson, B.E. (2017), "Biofuel blending reduces particle emissions from aircraft engines at cruise conditions", *Nature*, **543**(7645), 411. <https://doi.org/10.1038/nature21420>.
- Mostafa, S.S. and El-Gendy, N.S. (2017), "Evaluation of fuel properties for microalgae *Spirulina platensis* bio-diesel and its blends with Egyptian petro-diesel", *Arab. J. Chem.*, **10**, S2040-S2050.

- <https://doi.org/10.1016/j.arabjc.2013.07.034>.
- Niesłony, P., Grzesik, W., Chudy, R. and Habrat, W. (2015), "Meshing strategies in FEM simulation of the machining process", *Arch. Civil Mech. Eng.*, **15**(1), 62-70. <https://doi.org/10.1016/j.acme.2014.03.009>.
- Rodrigo, C.L., Manoel, F.N. and Danielle, R.G. (2017), "CFD modeling of a small-scale cyclonic combustor chamber using biomass powder", *Energy Procedia*, **120**, 556-563. <https://doi.org/10.1016/j.egypro.2017.07.208>.
- Rodrigues, L.O., Alencar, H.S., Nascimento, M.A. and Venturini, O.J. (2007), "Aerodynamic analysis using CFD for gas turbine combustion chamber", *ASME 2007 Power Conference, American Society of Mechanical Engineers*, **42738**, 547-557.
- Sabnis, P. and Aggarwal, S.K. (2018), "A numerical study of NOx and soot emissions in methane/n-heptane triple flames", *Renew. Energy*, **126**, 844-854. <https://doi.org/10.1016/j.renene.2018.04.007>.
- Sapp, M. (2017), "Airbus offering customers aircraft delivery using 10% aviation biofuel blend", *BiofuelsDigest*.
- Shokravi, H., Shokravi, Z., Heidarzadei, M., Ong, H.C., Kolor, S.S.R., Petru, M., ... & Ismail, A.F. (2021), "Fourth generation biofuel from genetically modified algal biomass: Challenges and future directions", *Chemosph.*, **285**, 131535. <https://doi.org/10.1016/j.chemosphere.2021.131535>.
- Singh, J. and Gu, S. (2010), "Commercialization potential of microalgae for biofuels production", *Renew. Sustain. Energy Rev.*, **14**(9), 2596-2610. <https://doi.org/10.1016/j.rser.2010.06.014>.
- Singh, P., S. K. Tiwari, et al. (2017), "Modification in combustion chamber geometry of CI engines for suitability of biodiesel: A review", *Renew. Sustain. Energy Rev.*, **79**, 1016-1033. <https://doi.org/10.1016/j.rser.2017.05.116>.
- Slade, R. and Bauen, A. (2013), "Micro-algae cultivation for biofuels: Cost, energy balance, environmental impacts and future prospects", *Biomass Bioenergy*, **53**, 29-38. <https://doi.org/10.1016/j.biombioe.2012.12.019>.
- Ved, K. and Padam, K. (2013), "Study of physical and chemical properties of biodiesel from sorghum oil", *Res. J. Chem. Sci.*, **3**(9), 64-68.
- Vennam, L.P., Vizuet, W., Talgo, K., Omary, M., Binkowski, F.S., Xing, J., ... & Arunachalam, S. (2017), "Modeled full-flight aircraft emissions impacts on air quality and their sensitivity to grid resolution", *J. Geophys. Res.: Atmosph.*, **122**(24). <https://doi.org/10.1002/2017jd026598>.
- Wang, W.C., Tao, L. et al. (2016), "Review of biojet fuel conversion technologies", NREL National Renewable Energy Laboratory, Golden.
- Wang, Y. and Chung, S.H. (2019), "Soot formation in laminar counterflow flames", *Progr. Energy Combust. Sci.*, **74**, 152-238. <https://doi.org/10.1016/j.pecs.2019.05.003>.
- Watanabe, H., Yamamoto, J.I. and Okazaki, K. (2011), "NOx formation and reduction mechanisms in staged O2/CO2 combustion", *Combust. Flame*, **158**(7), 1255-1263. <https://doi.org/10.1016/j.combustflame.2010.11.006>.
- Won, J., Baek, S.W., Kim, H. and Lee, H. (2019), "The viscosity and combustion characteristics of single-droplet water-diesel emulsion", *Energi.*, **12**(10), 1963. <https://doi.org/10.3390/en12101963>.
- Yi, T.H., Turangan, C., Lou, J., Wolanski, P. and Kindracki, J. (2009), "A three-dimensional numerical study of rotational detonation in an annular chamber", *47th AIAA Aerospace Sciences Meeting Including the New Horizons Forum and Aerospace Exposition*, January.
- Zhang, H. and Chen, W. (2015), "The role of biofuels in China's transport sector in carbon mitigation scenarios", *Energy Procedia*, **75**, 2700-2705. <https://doi.org/10.1016/j.egypro.2015.07.682>.
- Zhang, M., Zhenbo, F.U., Yuzhen, L. and Jibao, L. (2012), "CFD study of NOx emissions in a model commercial aircraft engine combustor", *Chin. J. Aeronaut.*, **25**(6), 854-863. [https://doi.org/10.1016/s1000-9361\(11\)60455-x](https://doi.org/10.1016/s1000-9361(11)60455-x).
- Zuber, M., Hisham, M.S.B., Nasir, N.A.M., Basri, A.A. and Khader, S.M.A. (2017), "A computational fluid dynamics study of combustion and emission performance in an annular combustor of a jet engine", *Pertanika J. Sci. Technol.*, **25**(3), 1019-1028.